Supporting Information

"Aerosol synthesized SWCNT networks with tuneable conductivity and transparency by dry transfer technique"

Antti Kaskela [a], *Albert G. Nasibulin* [a*], *Marina Y. Timmermans* [a], *Brad Aitchison* [b], *Alexios Papadimitratos* [c], *Ying Tian* [a], *Zhen Zhu* [a], *Hua Jiang* [a], *David P. Brown* [b] *Anvar Zakhidov* [d] *and Esko I. Kauppinen* [a,e*]

[a] NanoMaterials Group, Department of Applied Physics and Center for New Materials, Aalto University, P.O.Box 15100, 00076, Espoo, Finland.

[b] Canatu Oy, Tekniikantie 21, FI-02150 Espoo, Finland.

[c] Solarno, Inc., 153 Hollywood Drive Coppell, TX-75019, USA.

[d] NanoTech Institute, University of Texas at Dallas, Richardson, TX-75083, USA.

[e] VTT Biotechnology, Biologinkuja 7, 02044, Espoo Finland.

[*] Corresponding authors:

Albert Nasibulin, albert.nasibulin@tkk.fi, Tel: +358 50 33 975 38, Fax: +358 9 451 3517.

Esko Kauppinen, esko.kauppinen@tkk.fi, Tel: +358 40 50 980 64 Fax**:** +358 9 451 3517.

1. Sample preparation

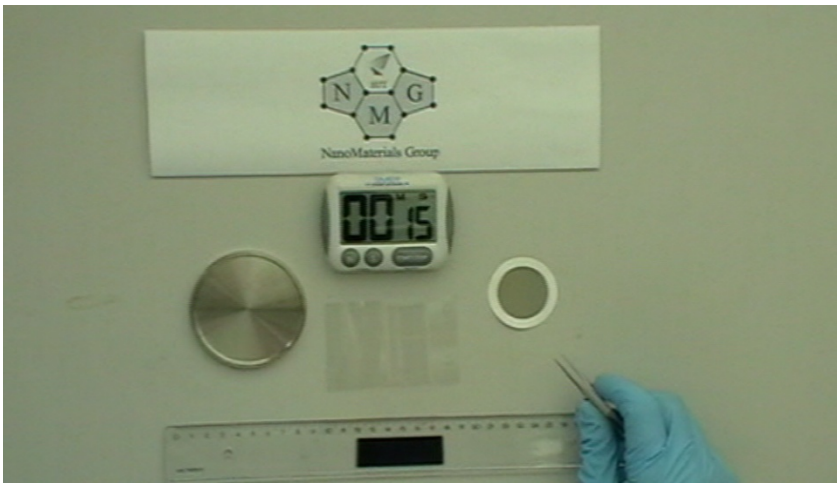

Movie S1 shows the procedure for the electrode preparation. The synthesized SWCNT-network, collected on a filter, can be transferred onto a flexible polymer substrate by a room temperature press transfer process. The PET-substrate (Bi-axially oriented, 125 μm thick, Goodfellow, Cambridge Ltd, England) and SWCNT-network on the filter were pressed together with a pressure of approximately 10^3 Pa. The applied pressure provides conformal contact and the SWCNT-network is adhered to the substrate. The membrane filter can be removed by lifting. The transfer process is extremely simple and no dispersion or cleaning steps are needed prior to press transfer. This makes the process significantly faster, cheaper and more environmentally friendly than traditional liquid based SWCNT-network deposition processes. The whole process for the preparation of a transparent electrode takes less than 15 s.

2. Flexibility demonstration

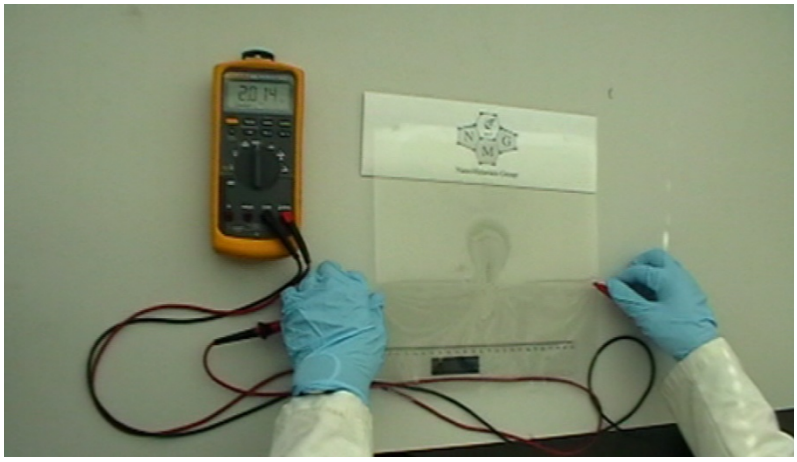

Movie S2 demonstrates the flexibility of a large area SWCNT-network with a transparency of 96 % on a PET-substrate (conductive area dimensions 28 cm × 28 cm). The film is flexed repeatedly without loss of electrical conductivity (resistance between two contacts is approximately 2 kΩ), which can be monitored by using a multi-meter (Fluke 87 V).

3. Capacitive touch sensor

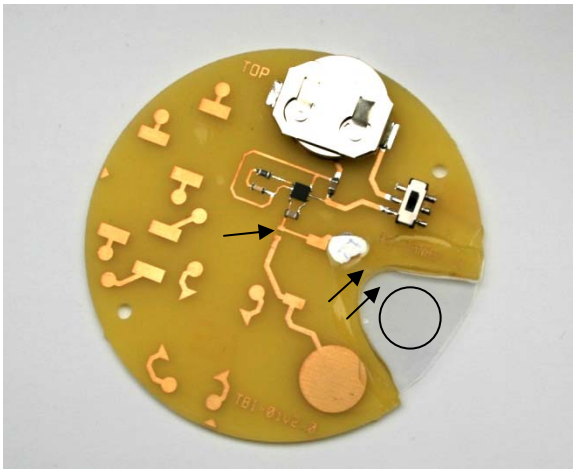

Movie S3 demonstrates a transparent, capacitive touch (proximity) sensor electrode, which utilizes a dry transferred SWCNT-network as a sensing element (transmittance 98%, sheet resistance 4 kΩ/□). The SWCNT-network sensor is located inside the black circle in the image. Transparent SWCNT-networks (indicated by arrows) are bridging the copper and the SWCNT electrodes. The readout electronics demonstrate their conductivity. In the video we activate the indicator light emitting diode (LED) with both the copper reference electrode and optically transparent SWCNT-network electrodes by placing a finger in a close proximity to the sensor. Control touches outside the active area do not trigger the LED. The used sensing circuit is built according the reference design from Atmel QT100A datasheets and it is schematically depicted in the figure S1.

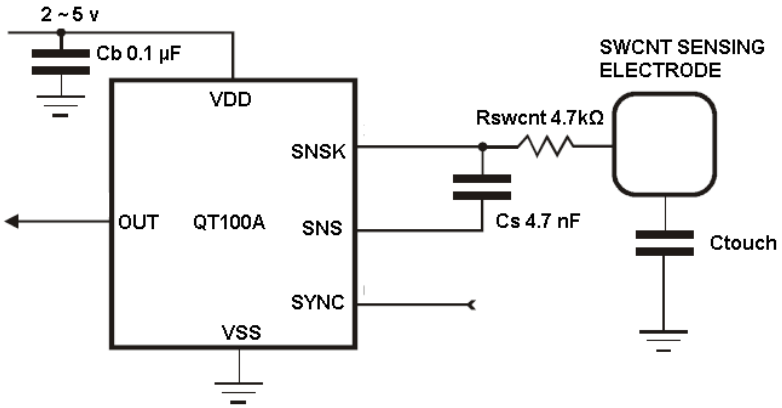

Figure S1. The electrical schematics of the capacitive touch sensor, which is based on the reference design from the datasheets of the Atmel QT100A IC, which was used for the presented device.

4. Electron and atomic force microscopy characterization of SWCNTs.

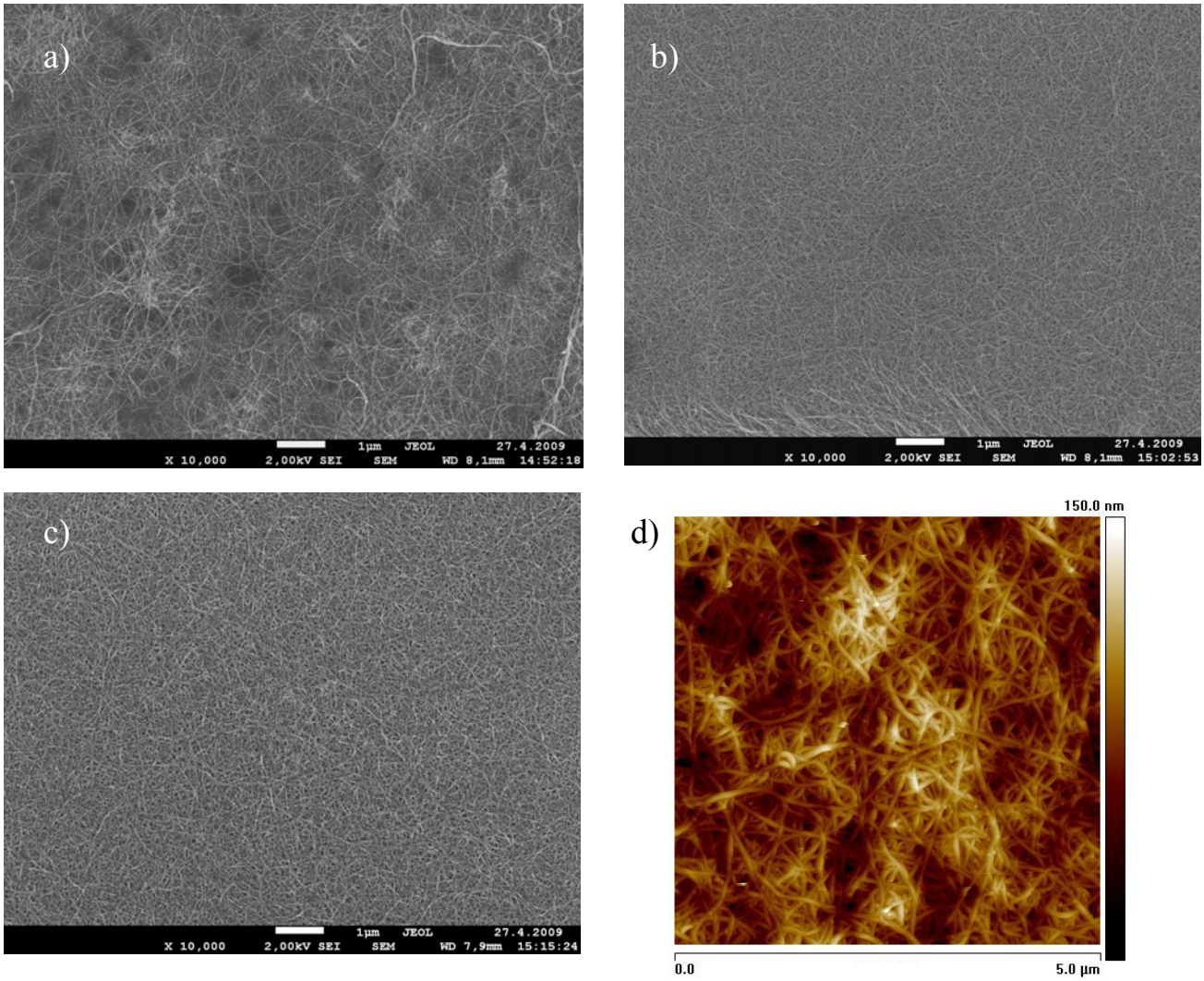

Figure S2. The effect of post-deposition liquid treatments is clearly visible in the morphology of SWCNT-electrodes by SEM imaging. The figure depicts a) the morphology of a pristine SWCNT-network, b) the morphology of ethanol treated and c) ethanol and HNO_3 treated SWCNT-electrodes on PET substrates. Network densification due to the liquid treatment is clearly visible from the micrographs as the number of SWCNT-layers within the focal length of the SEM increases. d) AFM-scan over a similar liquid treated SWCNT-electrode.

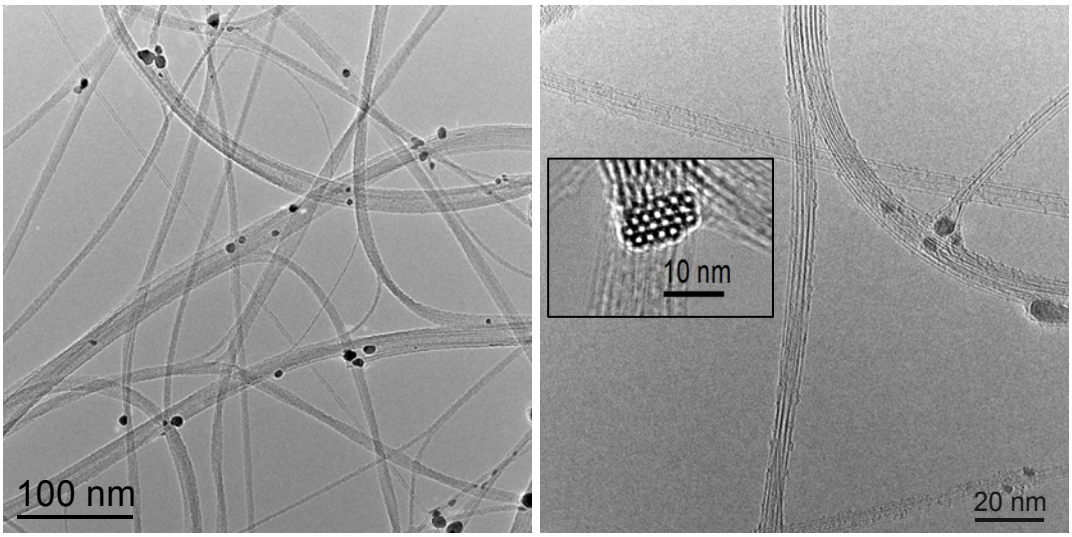

Figure S3. Typical TEM images of SWCNTs with the bundle length of 9.4 µm produced in a scaled-up version reactor. Inset shows a cross-section of a bundle.

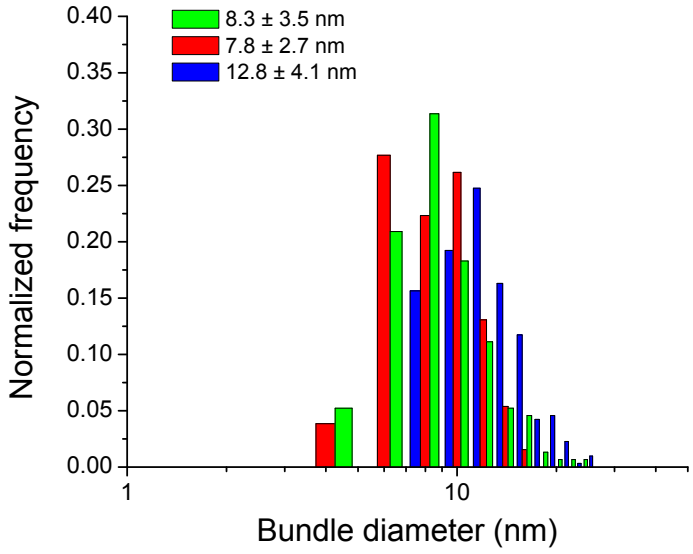

Figure S4. The log-normal bundle diameter distributions obtained on the basis of statistical measurements from TEM images. The geometric mean bundle diameters are 8.3 ± 3.5 nm, 7.8 ± 2.7 nm and 12.8 ± 4.1 nm corresponding to bundle lengths of 1.3, 3.3 and 9.4 µm.

5. Examples of SWCNT deposits on various substrates.

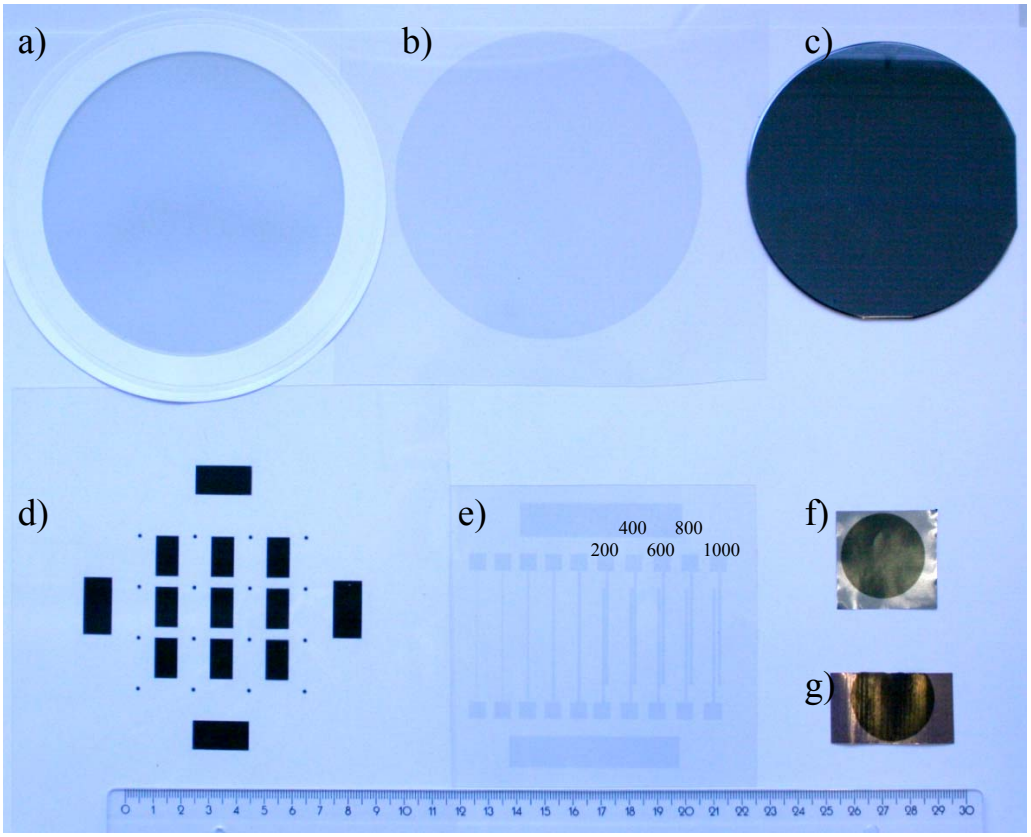

Figure S5. A photograph of various substrates with dry transferred SWCNT-networks: a) a filter covered by SWCNTs after filtering the flow at the outlet of the reactor; b) SWCNT-network film on PET; c) a silicon wafer fully covered by SWCNT-network; d) and e) SWCNT-networks patterned using masks under the filter and transferred to PET. The number shows the distance between electrodes in μm. SWCNT-network on f) Fe and g) Cu foils.

6. Post-deposition treatment of SWCNTs.

In order to increase the conductivity of the SWCNT films we developed a fast post-deposition treatment. The SWCNT-network is first densified by drop casting of ethanol (Etax Aa, Altia, Finland) and subsequently dried in ambient lab atmosphere. As the ethanol evaporates from a SWCNT-network surface, the surface tension of the ethanol compresses the SWCNT-network in the out-of-plane direction. The densification is followed by 60 s dipping in concentrated nitric acid (65 % HNO_3, J. T. Baker, Netherlands) and de-ionized water rinsing for 15 s. The sheet resistance and optical characterizations were performed after 1 h storage in ambient conditions.

It was found that even only 1 min HNO_3 treatment of SWCNTs led to significant changes in the optical absorption and Raman spectra (Fig. 1b and 1c). These can be explained by p-type doping of the SWCNTs as shown in Figure S6. Changes in the absorption spectra (Fig. 1b) show nitric acid treatment caused the elimination of the absorption peaks of the S_{11} and S_{22} transitions of the semiconducting tubes and a small decrease of the M_{11} peak from the metallic tubes. This indicates a shift in the Fermi level, E_F (Figure S6). Since the valence bands V_1 and V_2 are empty, the semiconducting SWCNTs cannot absorb photons by the energy transition from the first (V_1) and second (V_2) levels of van Hove singularities in the valence band to, respectively, the first (C_1) and second (C_2) conduction band levels. For metallic tubes, the decrease in the absorption intensity means that some metallic tubes (with larger diameters and therefore smaller energy separation between V_1 and C_1) are also doped so that the Fermi level is lower than the first valence band (V_1).

Similarly, this interpretation of the doping of SWCNTs can be confirmed by Raman results. As has been recently shown, the shift of the tangential G band in the Raman spectra provides evidence of doping[1,2]. A shift to lower frequencies occurs due to n-type doping (electron-donor dopants) and to higher frequencies due to p-type (electron-acceptor dopants). These shifts indicate charge transfer between the dopants and the SWCNTs. The difference in Raman spectra obtained

from pristine and HNO_3 treated SWCNT-networks reveal a substantial up-shift of the G-band (Fig.1c) and therefore indicate p-type doping. Complete or partial disappearances of RBM bands indicate that all or some of the doped SWCNTs lost resonance enhancement. This could be related to the quenching of interband absorption due to the shift of the Fermi level. Larger tubes having smaller band gap would result in the greater quenching for a given shift of E_F. Thus, only very weak peaks at around 195 and 220 cm^{-1} corresponding to small diameter tubes are observed in the Raman spectra of acid treated samples.

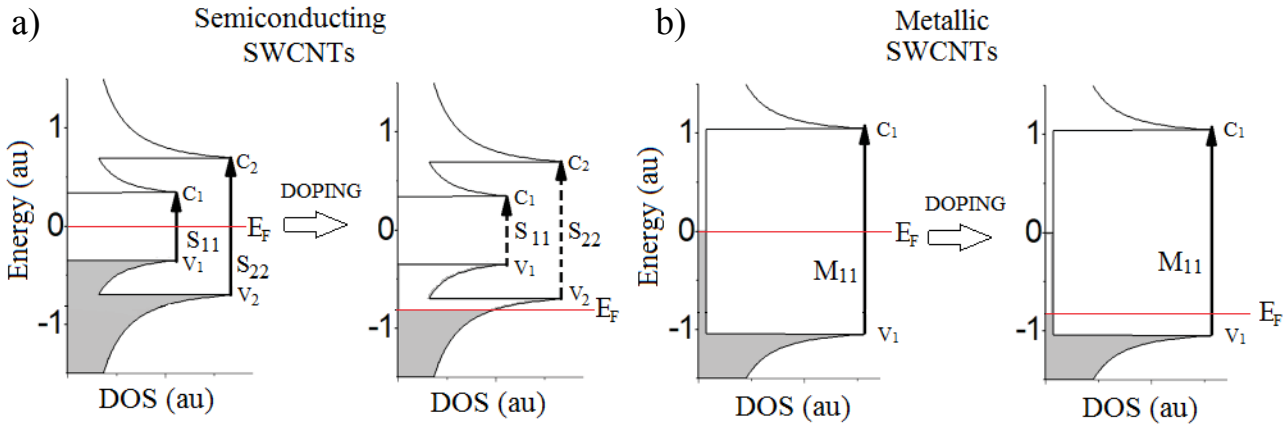

Figure S6. Schematic presentation of the change in density of states (DOS) due to HNO_3-treatment for both a) semiconducting and b) metallic SWCNTs.

7. SWCNT thin film transistor fabrication

The dry transfer technique was successfully applied for the deposition of both high and low density homogeneous SWCNT films. This opens possibilities for a broad field of applications, allowing the utilization of the films with metallic or semiconducting properties depending on the SWCNT density. One of the potential applications is the use of sparse SWCNT networks as a semiconducting material for the fabrication of thin film transistors (TFTs). The application of low density SWCNT-networks as TFT channels has been shown to exhibit the higher performance, in comparison to organic TFTs, and potentially low-cost fabrication [3-5]. Dry transfer deposition of SWCNT-networks is advantageous over existing printing and spraying methods since it is performed in a simple one-step low-cost process and no mechanical or chemical treatments are used. Bottom-gate transistor structures have been fabricated to demonstrate the applicability of the dry transfer deposition method for the fabrication of TFTs.

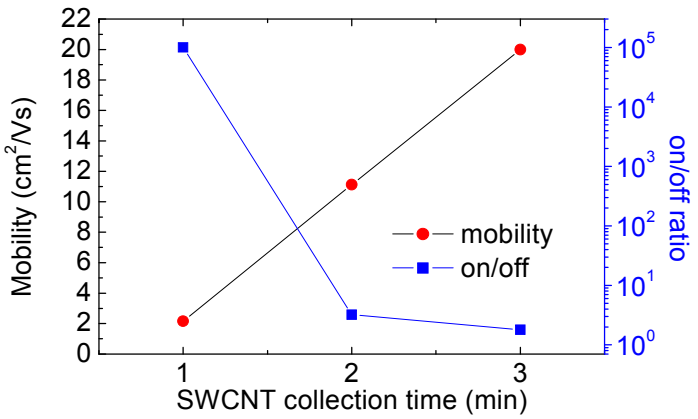

Figure S7. The relationship between mobility and on-off-ratio in SWCNT-network transistors with various SWNCT densities depending on the SWCNT collection time.

A thin SWCNT film, collected onto a nitrocellulose filter for a short period of time (typically 10 s - 3 min) directly downstream of the laboratory scale reactor, was transferred by pressing the

filter against a highly boron-doped Si substrate covered with a thermally grown SiO_2 layer (100 nm). The SiO_2 acts as the gate dielectric. A thin Al layer was sputtered on the back-side of the Si substrate to ensure good contact for the back-gate electrode. Source and drain electrodes (5 nm Ti/ 45 nm Au) were deposited using an electron-beam evaporator (IM9912) by standard photolithography and lift-off techniques. The SWCNT-network was patterned by means of O_2 plasma etching (channel length 10 um and channel width 50 um). For this, photolithography was employed in order to produce the etch mask from photoresist, thus protecting the transistor channel.

To study the reproducibility of the SWCNT-transistor channels a separate sample set consisting of 17 transistors was fabricated and characterized. These transistors had channel dimensions of 50 μm × 50 μm and shared the 100 nm gate oxide. The reproducibility was found to be at acceptable level, as both the mobility and on/off ratio had standard deviations of 40%.

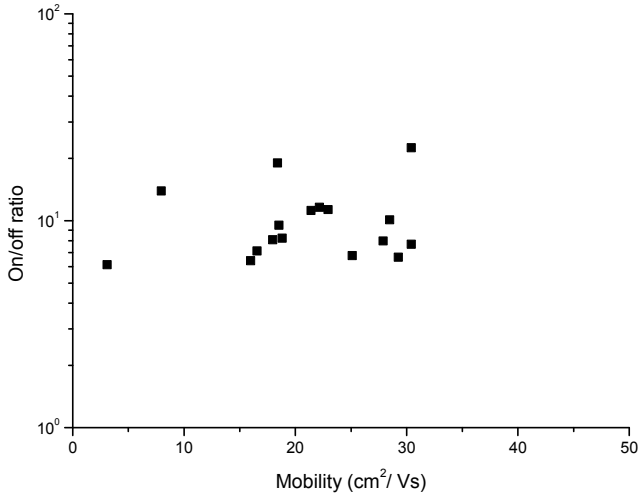

Figure **S8**. Mobility vs. on/off ratio of set of 17 transistors fabricated by dry transfer technique.

8. Fabrication of bright OLEDs with SWCNT electrodes.

OLEDs need transparent electrodes with high work function, such as conventional ITO. Multiwalled CNT (MWCNT) sheets dry drawn from oriented CVD forests have been used for bright OLEDs.[6] However, MWCNT sheets are made of large diameter nanotubes, which are not very flexible at small scales and may act mechanically as strong needles that can electrically short the thin emissive layer (typical thickness of a few 100 nm). Also, it was found that MWCNT sheets dry spun from CVD forests are usually too dense, and create a very high injection current of holes. This decreases the lifetime of OLEDs with dense CNT networks (although they are good for achieving brightness above 4500 cd/m^2). It was found also that very low density MWCNT networks, unintentionally created during spin-coating[6] on the sides around main pixels, can produce bright electroluminescent light and are sufficient for the device operation. Therefore, one significant advantage of our present dry transfer technique is that it allows one to create very low density networks, which are most appropriate for balanced injection of holes in OLEDs, increasing their lifetime significantly. Another major advantage is the extremely flexible character of thin SWCNTs, due to which the network is more like wet noodles (rather than sharp MWCNT chop sticks). Due to this elasticity it is easier to built OLEDs without electrical shorting to the cathode.

The OLED configuration is shown in Figure S9. SWCNT sheets were transferred on top of glass substrates and densified with ethanol. A layer of poly(3,4-ethylenedioxythiophene) poly(styrenesulfonate) (PEDOT:PSS type CLEVIOS PH) was spin cast on top of the SWCNT at 4000 rpm. Prior to the coating of the active layer, the samples were annealed on a hot plate at 140 ^{o}C for 10 minutes. The active layer was also spin cast at 1000 rpm and annealed at 140 ^{o}C for 5 minutes before the cathode deposition. Finally, 100 nm of Al were evaporated through a shadow mask to form the cathode. Before the Al deposition, a thin layer of $CsCO_3$ was applied on the emissive layer

to enhance electron injection from the cathode. All characterizations were done using a Keithley 236 source measurement unit and a Photo Research PR-650 Spectracolorimeter. Typical spectra of the emission of blue and orange OLEDs with SWCNT hole injectors are shown below.

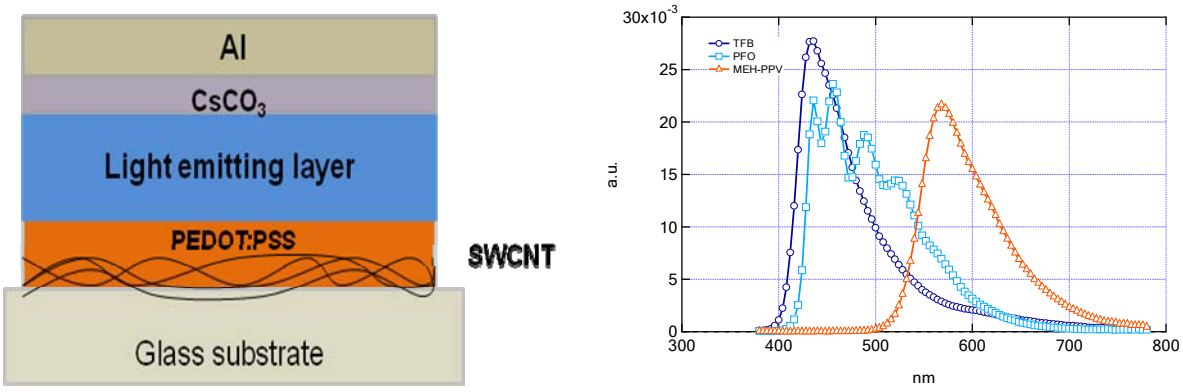

Figure S9. OLED device schematic and emission spectrum of devices with different emissive layers.

9. Uniformity of the SWCNT electrodes and sample reproducibility

Spatial uniformity and reproducibility are both important factors when considering electronics applications of large area SWCNT-network electrodes. The uniformity of SWCNT-electrodes was characterized by measuring the electrical sheet resistance and optical transmittance at 550nm wavelength at 9 different locations on round SWCNT-electrode of 110 mm in diameter. The sample treated by the ethanol and concentrated nitric acid treatments as described previously in this text. Typical optical and electrical characterization results are shown in the figure S10 and a photograph of a round SWCNT-electrode is shown in the Fig. S5b. The samples were found to be reasonable uniform both optically and electrically. The maximum variation of optical transmittance was found to be 0.5 % from the average which is in close agreement with the precision of 1 % of the spectrophotometer. For the electrical sheet resistance the maximum variation was found to be 7 % which is near the measurement precision of 5%. Sample reproducibility was studied analysing a series of 6 consecutive samples which were collected in 30 min intervals for constant deposition duration of 17 min. The sample to sample variation of the average optical transmittance and sheet

resistance were at found to be comparable with the measurement precision as presented in the figure S11.

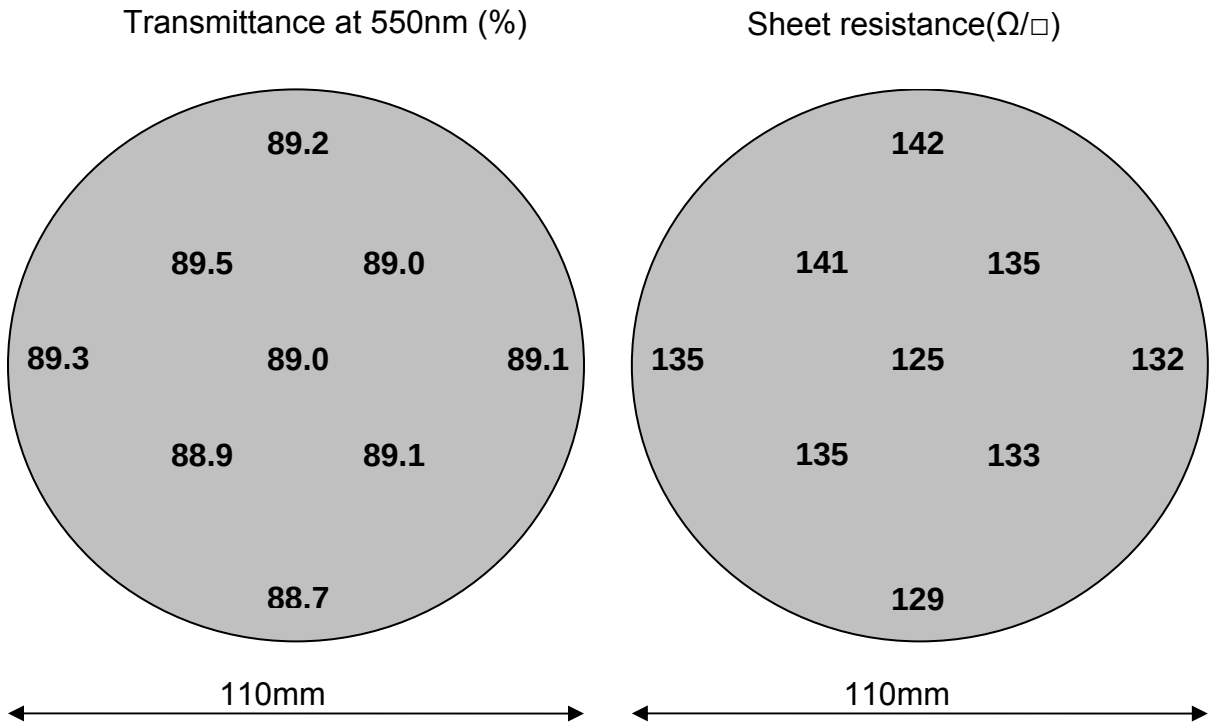

Figure S10. Spatially resolved optical transmittance and electrical sheet resistance measurements on a round SWCNT-electrode of 110 mm in diameter. The maximum variations were found to be around 0.5% and 7 % for optical transmittance at 550nm and for sheet resistance, respectively.

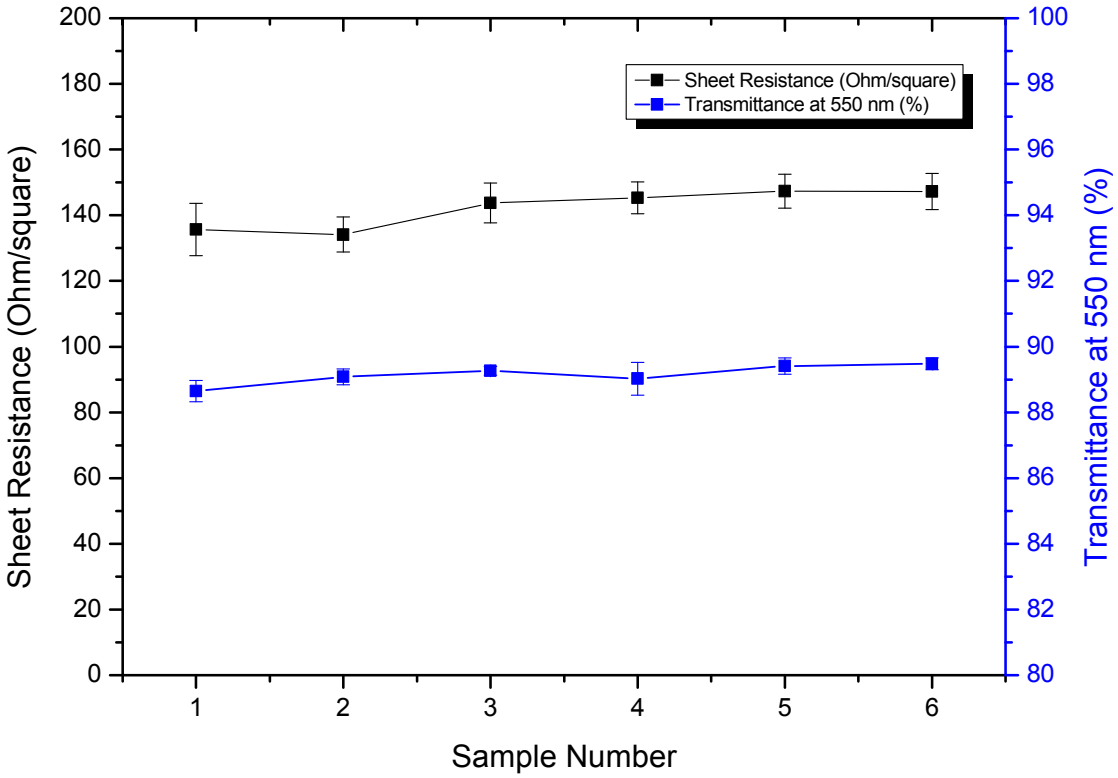

Figure S11. The reproducibility of sheet resistance and transmittance. The samples are collected at 30 min intervals. The average values of both the sheet resistance and the optical transmittance are overlapping within the error bounds which are estimated by the standard deviation of the 9 averaged measurement points on the sample surface.

References

1) Geng, H. Kim, K.K. So, K.P. Lee, Y.S, Chang, Y. & Lee, Y.H. Effect of Acid Treatment on Carbon Nanotube-Based Flexible Transparent Conducting Films. *J. Am. Chem. Soc.* **129,** 7758-7759 (2007).

2) Lee, R. S. Kim, H. J. Fischer J. E., Thess, A. & Smalley R. E. Conductivity enhancement in single-walled carbon nanotube bundles doped with K and Br. *Nature* **388,** 255-257 (1997).

3) Snow, E. S. Novak, J. P. Campbell, P. M. & Park D. Random networks of carbon nanotubes as an electronic material. *Appl. Phys. Lett.,* **82,** 2145-2147 (2003).
4) Artukovic E., Kaempgen, M. Hecht, D.S. Roth, S. & Gruner, G. Transparent and flexible carbon nanotube transistors. *Nano Lett,* **5,** 757-760 (2005).
5) Zavodchikova, M.Y. Kulmala, T. Nasibulin, A.G. Ermolov, V. Franssila, S. Grigoras, K. & Kauppinen, E.I. Carbon nanotube thin film transistors based on aerosol methods. *Nanotechnology*, **20,** 085201 (2009).
6) Williams, C. D. Robles, R.O. Zhang, M. Lee, S. Baughman, R.H. & Zakhidov, A.A. Multiwalled carbon nanotube sheets as transparent electrodes in high brightness organic light-emitting diodes. *Appl. Phys. Lett.* **93,** 183506 (2008).